AIP | Applied Physics Letters

Toward terahertz heterodyne detection with superconducting Josephson junctions

M. Malnou, A. Luo, T. Wolf, Y. Wang, C. Feuillet-Palma et al.

Citation: Appl. Phys. Lett. **101**, 233505 (2012); doi: 10.1063/1.4769441
View online: http://dx.doi.org/10.1063/1.4769441
View Table of Contents: http://apl.aip.org/resource/1/APPLAB/v101/i23
Published by the American Institute of Physics.

Toward terahertz heterodyne detection with superconducting Josephson junctions

M. Malnou,[1] A. Luo,[1] T. Wolf,[1] Y. Wang,[1] C. Feuillet-Palma,[1] C. Ulysse,[2] G. Faini,[2] P. Febvre,[3] M. Sirena,[4] J. Lesueur,[1] and N. Bergeal[1]
[1]*Laboratoire de Physique et d'Etude des Matériaux-UMR8213-CNRS-ESPCI ParisTech-UPMC, 10 Rue Vauquelin, 75005 Paris, France*
[2]*Laboratoire de Photonique et de Nanostructures LPN-CNRS, Route de Nozay, 91460 Marcoussis, France*
[3]*IMEP-LAHC-UMR 5130 CNRS, Université de Savoie, 73376 Le Bourget du Lac cedex, France*
[4]*Centro Atómico Bariloche, Instituto Balseiro CNEA and Univ. Nac. de Cuyo, Av. Bustillo 9500, 8400 Bariloche, Rio Negro Argentina*

(Received 20 June 2012; accepted 14 November 2012; published online 5 December 2012)

We report on the high-frequency mixing properties of ion irradiated $YBa_2Cu_3O_7$ Josephson junctions. The frequency range, spanning above and below the characteristic frequencies f_c of the junctions, permits a clear observation of the transition between two mixing regimes. The experimental conversion gain was found to be in good agreement with the prediction of the three-port model. Finally, we discuss the potential of the junctions to build a Josephson mixer operating in the terahertz frequency range. © *2012 American Institute of Physics*.
[http://dx.doi.org/10.1063/1.4769441]

The terahertz (THz) region of the electromagnetic spectrum [0.3–10 THz] has so far not been exploited fully because of the lack of suitable sources and detectors.[1] Indeed, THz frequencies lie between the frequency range of traditional electronics and photonics where the existing technologies cannot be simply extended. Low temperature superconductor-insulator-superconductor Niobium tunnel junctions are currently used as a frequency-mixing element in heterodyne receivers,[2] providing extremely low noise and high sensitivity.[3] However, these junctions are intrinsically limited in frequency by the energy gap of Nb (~800 GHz) and operate only at low temperature (4.2 K).

An alternative to these devices is to use high-temperature superconducting (HTS) receivers based on Josephson junction mixers or hot-electron bolometers. In addition to the obvious advantage of a much higher operating temperature, the investigation of HTS mixers is motivated by the possibility of approaching quantum-limited noise performance at frequencies higher than what is possible with conventional Nb devices.[4,5] Hence, it is important to develop HTS devices and related heterodyne mixer technology for applications in the THz range. However, despite a few promising realizations mainly based on grain-boundary or ramp edge junctions,[6–9] the development was slowed down by the difficulty to build a junction technology sufficiently reliable to fabricate complex devices. In recent years, an approach based on ion irradiation has been developed to make Josephson junctions with high temperature superconductors. This method has been used to make reproducible junctions,[10,11] superconducting quantum interference devices (SQUIDs),[12] and large-scale integrated Josephson circuits.[13,14] In this letter, we report on a study of the high-frequency mixing properties of Josephson junctions made by this technique.

Fig. 1(a) shows an optical picture of a Josephson junction embedded in a self-complementary THz spiral antenna. We used 70 nm thick $YBa_2Cu_3O_7$ films grown on sapphire substrates. The junction is defined in a 2 μm wide superconducting channel by irradiating through a 20 nm wide slit with 100 keV oxygen ions at a fluence of 3×10^{13} at/cm^2. The fabrication method has been described in detail in Ref. 15. The junction is connected to contact pads for dc biasing and to a microwave transmission line to read the output signal. The back side of the sapphire substrate is placed in contact with a silicon hyper-hemispheric lens located at the focal point of a parabolic mirror exposed to external signals through the window of the cryostat. A cryogenic HEMT

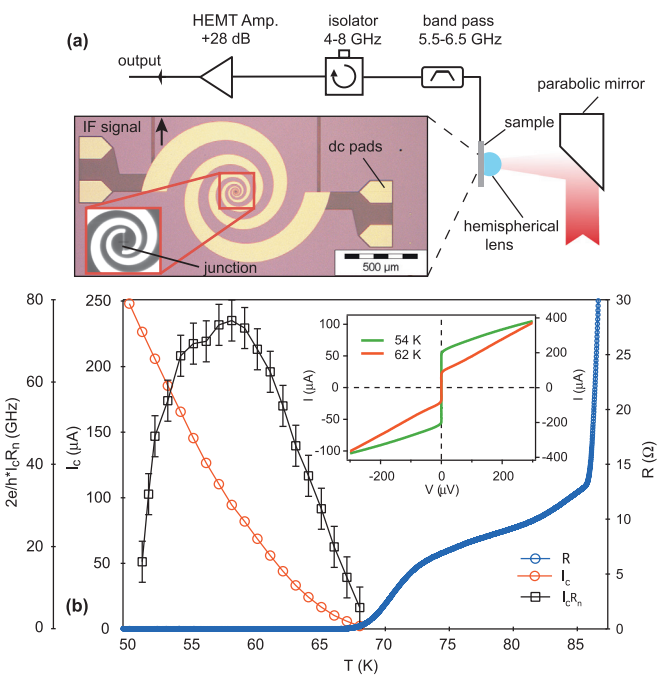

FIG. 1. (a) Josephson mixer in its optical and microwave set-up. The junction is embedded in a wide-band spiral antenna (85 GHz-7 THz). (b) Resistance, critical current, and I_cR_n product of the junction as a function of temperature. (Inset) I(V) curves at two temperatures below and above T_c' showing the difference between the Josephson regime (upward curvature) and the flux flow regime (downward curvature).

amplifier [4–8 GHz] amplifies the output signal at the intermediate frequency (IF) before further amplification at room temperature. An isolator is placed in the chain to minimize the back-action of the amplifier on the Josephson mixer.

The resistance of the junction as a function of temperature is shown in Fig. 1(b). The highest transition refers to the superconducting transition of the reservoirs (i.e., non irradiated electrodes) at $T_c^0 = 85\,\mathrm{K}$, which corresponds to the transition temperature of the unprocessed $YBa_2Cu_3O_7$ film.[10] The second transition at the lower temperature $T_J = 68\,\mathrm{K}$ corresponds to the occurrence of the Josephson coupling between the two electrodes, and not to the transition of the irradiated part itself that is expected at the lower temperature $T_c' \approx 52\,\mathrm{K}$. Junctions fabricated by this method are in the low capacitance regime, defined by a McCumber dimensionless parameter $\beta_c = \frac{2e}{\hbar} I_c R_n^2 C$ much smaller than one[16] (I_c is the critical current, R_n the normal-state resistance, and C the capacitance of the junction). Junctions have non-hysteretic current-voltage characteristics with an upward curvature of the dissipation branch and no sharp feature at the gap voltage (Fig. 1(b) inset), a behavior well described by the resistively shunted junction (RSJ) model.[16]

Below T_J, the critical current I_c increases with a quadratic law when the temperature is lowered (Fig. 1(b)). At the lower temperature T_c', the junction enters a flux-flow regime and the I(V) characteristics display a downward curvature (inset Fig. 1(b)). The characteristic frequency f_c of the junction is defined by the I_cR_n product via the Josephson frequency $f_c = (2e/h)I_cR_n$. Although the mixing operation is optimal when the signal frequency is lower than f_c, it can be performed up to frequencies corresponding to several times the value of f_c with a reduced conversion efficiency. As can be seen in Fig. 1(b), the characteristic frequency of the junction is temperature-dependent and takes a maximum value $f_c^{\max} = 75\,\mathrm{GHz}$ at 58 K. The decrease of f_c below this temperature is due to the drop in R_n as the temperature approaches the flux flow regime.

The observation of Shapiro steps is important to evaluate the dynamic properties of a Josephson junction.[17] I(V) characteristics under 20 GHz radiation have been measured as a function of radiation power. Figure 2(a) shows the differential resistance of the junction $\frac{dV}{dI}$ as a function of bias current and power radiation. The oscillations of several Shapiro steps with power can be clearly observed here. The data are in qualitative agreement with the predictions of the current driven RSJ model, which admits a single parameter f_c (Figs. 2(b) and 2(c)).

To study the mixing properties of the junction, a strong local oscillator signal at frequency f_{LO} and a weaker test signal at frequency f_s are injected through the optical window of the cryostat. Three main ranges of frequency have been investigated: (i) $f_{\mathrm{LO}} = 20\,\mathrm{GHz} < f_c^{\max}$, (ii) $f_{\mathrm{LO}} = 70\,\mathrm{GHz} \approx f_c^{\max}$, and (iii) $f_{\mathrm{LO}} = 140\,\mathrm{GHz} > f_c^{\max}$. Figs. 3(a)–3(c) show the output power measured at the IF $f_{\mathrm{IF}} = |f_{\mathrm{LO}} - f_s| = 5.5\,\mathrm{GHz}$ as a function of the dc voltage V across the junction for these three ranges. In these measurements, the power of the local oscillator has been set to reduce the critical current to approximately half of its value as it corresponds to an optimal operation point for mixer performances. In the regime $f_{\mathrm{LO}} < f_c^{\max}$, the power at f_{IF} displays maxima located at the center of each Shapiro step (Fig. 3(a)), whereas in the regime $f_{\mathrm{LO}} > f_c^{\max}$ there are two maxima within a Shapiro step, separated by a dip at the center (Fig. 3(c)). The regime $f_{\mathrm{LO}} \approx f_c^{\max}$ corresponds to an intermediate situation where the power at f_{IF} is approximately flat at the center of the steps (Fig. 3(b)). The output power at the IF was measured as a function of the signal power for the three ranges of frequency. The mixer displays a linear dynamical range of more than 55 dB at 20 GHz and 30 dB at 140 GHz (supplementary Figure 1 (Ref. 18)). Measurements performed at higher frequencies, $f_{\mathrm{LO}} = 280$ and 410 GHz (Figs. 3(d) and 3(e)) indicate that the junction can response in the lower part of the THz range. However, in this case, the power of the source was not sufficient to reach optimal bias conditions. Mixing at frequency higher than 410 GHz was not investigated in this study.

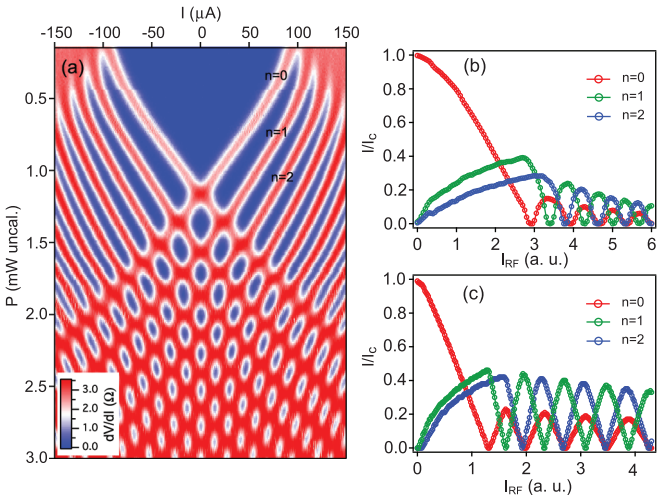

FIG. 2. (a) Differential resistance of junction (color scale) under a 20 GHz signal as a function of bias current and signal power. (b) Experimental height of the n = 0, n = 1, and n = 2 Shapiro steps as a function of signal current measured at T = 58 K. (c) Theoretical height of the n = 0, n = 1, and n = 2 Shapiro steps as a function of signal current obtained from the RSJ model.

The three-port model has been used in the context of the RSJ model to calculate the theoretical performance of the mixer.[4,19] It describes the linear response due to a small signal by solving the non-linear response of the mixer to the local oscillator illumination. Only three frequencies of relevance are considered: the upper side-band (USB) $f_{\mathrm{LO}} + f_{\mathrm{IF}}$, the lower side-band (LSB) $f_{\mathrm{LO}} - f_{\mathrm{IF}}$, and the intermediate frequency f_{IF}. The frequency conversion matrix is defined by

$$\begin{pmatrix} V_u \\ V_0 \\ V_l^* \end{pmatrix} = \begin{pmatrix} Z_{uu} & Z_{u0} & Z_{ul} \\ Z_{0u} & Z_{00} & Z_{0l} \\ Z_{lu} & Z_{l0} & Z_{ll} \end{pmatrix} \begin{pmatrix} I_u \\ I_0 \\ I_l^* \end{pmatrix},$$

where u, l, and 0 stand for USB, LSB, and IF respectively, and V_j and I_i are the voltages and currents at those respective frequencies. Each element Z_{ij} is simply the ratio of the voltage at the relevant frequency V_j with the current injected I_j. The diagonal elements are the impedances of the junction at the corresponding frequencies, whereas the off-diagonal elements give the non-linearity necessary for mixing. The matrix elements can be calculated by including a small signal in the RSJ model pumped by the LO signal. The

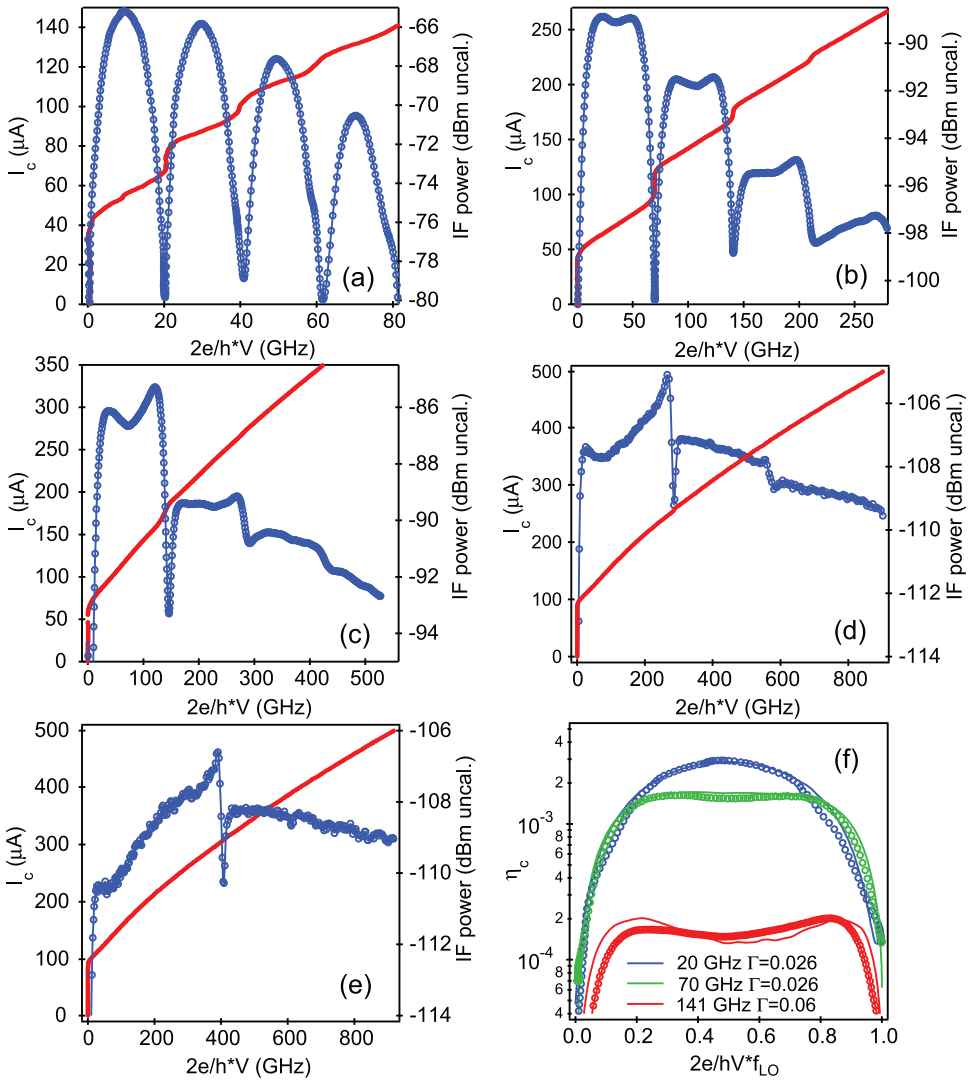

FIG. 3. (a)-(e) Output power at the intermediate frequency (right scale) and dc current (left scale) as a function of voltage for five different LO frequencies, $f_{LO} = 20$ GHz (a), $f_{LO} = 70$ GHz (b), $f_{LO} = 140$ GHz (c), $f_{LO} = 280$ GHz (d), $f_{LO} = 410$ GHz (e). The IF frequency is 5.5 GHz. For the three lowest frequencies (panels (a)-(c)), the power of the signal has been set to approximately one thousandth of the power of the local oscillator. For the two highest frequencies (d) and (e), the signal power is of the same order as the LO one. (f) Comparison between experimental (dots) and theoretical (full lines) conversion efficiency η_C for the three lowest frequencies. The noise parameter Γ used for the calculation is indicated on the figure.

thermal noise is included in the model by the addition of an uncorrelated Gaussian distributed random current fluctuation of variance $\sigma^2 = \Gamma/\Delta\tau$, where $\Gamma = 2ek_BT/\hbar I_c$ is the dimensionless RSJ noise parameter and $\Delta\tau$ is the normalized time step. To take into account thermal noise, the matrix is calculated for each value of the bias current and averaged over many realizations. To determine the conversion efficiency, we introduce the external part of the circuit described by the diagonal impedance matrix Z_{ext} whose elements Z_u, Z_l, and Z_0 are connected to the mixer inputs. Here, Z_u and Z_l represent the impedance of the spiral antenna (80 Ω) and are taken to be identical. Z_0 is the 50 Ω impedance of the microwave readout line. The conversion efficiency is defined as the ratio of the IF power dissipated in the impedance Z_0 to the available test signal power on Z_u (or Z_l); it can be derived from the conversion matrix[19]

$$\eta_c = 4 * \Re(Z_u)\Re(Z_0)|Y_{0u}|^2, \quad (1)$$

where Y_{0u} is the matrix element of the Y matrix defined by $Y = (Z + Z_{ext})^{-1}$.

As shown in Fig. 3(f), the experimental data are in good agreement with the theoretical calculations derived from the three-port model.[19] In particular, it describes well the crossover from the first regime $f_{LO} < f_c^{max}$ to the second regime $f_{LO} > f_c^{max}$. For $f_{LO} = 20$ GHz and 70 GHz, the noise parameter Γ was taken to be 0.026 corresponding to a critical current of 100 μA at 58 K. For $f_{LO} = 140$ GHz, it was not possible to reach a quantitative agreement with $\Gamma = 0.026$. The best fit, shown in the figure, was obtained for $\Gamma = 0.06$ indicating that the junction is submitted to an extra noise, equivalent to an effective temperature twice larger than the physical one. The conversion efficiency takes a maximum value of 0.3% at 20 GHz and decreases to 0.02% at 140 GHz. Its overall weak absolute value is due to the low impedance of the junction (2Ω) compared to the external impedances Z_u and Z_0. This problem can be overcome by modifying the geometry of the junction. In principle, the impedance of the junction can be increased easily up to 20 Ω by changing both the width and the thickness of the junction, leading to a much higher conversion efficiency.

The junction presented in this study has a characteristic frequency which is lower than the ones usually reported in grain-boundary junctions.[6–9] However, several developments can be made to optimize the I_cR_n product[20,21] in our junctions. In particular, a higher fluence of irradiation combined with an annealing of the sample should lead to a qualitative improvement.[22,23] Let us also mention that junctions made recently by irradiation through larger slits display f_c values up to 500 GHz (supplementary Figure 2 (Ref. 18)). This is a

promising result although their mixing properties have not been measured yet.

In conclusion, we have demonstrated the mixing operation of ion-irradiated $YBa_2Cu_3O_7$ Josephson junctions up to 420 GHz at 58 K. We have clearly shown the transition between the two mixing regimes, $f_{LO} < f_c^{max}$ and $f_{LO} > f_c^{max}$, in good agreement with the three-port RSJ model. In the short term, characteristic frequencies of order 500 GHz at $T > 40$ K are entirely within reach enabling mixing operation up to $\sim$1 THz. In addition, the natural scalability of the ion irradiation technique[14] makes it particularly interesting to implement, next to the mixer, an integrated Josephson local oscillator made of an array of junctions and whose frequency could be tuned by dc biasing.[24,25]

The authors thank L. Olanier for technical support. This work was supported by the international cooperation program MINCyT-ECOS A10E05, the Emergence program Contract of Ville de Paris and by the Région Ile-de-France in the framework of CNano IdF and Sesame program and by the PEPS NANANA of CNRS. CNano IdF is the nanoscience competence center of the Paris Region, supported by CNRS, CEA, MESR and Région Ile-de-France.

[1]M. Tonouchi, Nature Photon. **1**, 97–105 (2007).
[2]T. De Graauw, F. P. Helmich, T. G. Phillips, J. Stutzki, E. Caux, N. D. Whyborn, P. Dieleman, P. R. Roelfsema, H. Aarts, R. Assendorp *et al.*, Astron. Astrophys. **518**, L6 (2010).
[3]C. A. Mears, Q. Hu, P. L. Richards, A. H. Worsham, D. E. Prober, and A. V. Räisänen, Appl. Phys. Lett. **57**, 2487–2489 (1990).
[4]R. J. Schoelkopf, Ph.D. dissertation, California Institute of Technology, Pasadena, 1995.
[5]J. H. Claassen and P. L. Richards, J. Appl. Phys. **49**, 4117 (1978).
[6]J. Chen, H. Myoren, K. Nakajima, T. Yamashita, and P. H. Wu, Appl. Phys. Lett. **71**, 707 (1997).
[7]J. Scherbel, M. Darula, O. Harnack, and M. Siegel, IEEE Trans. Appl. Supercond. **12**, 1828 (2002).
[8]O. Harnack, M. Darula, S. Beuven, and H. Kohlstedt, Appl. Phys. Lett. **76**, 1764 (2000).
[9]M. Tarasov, E. Stepantsov, D. Golubev, Z. Ivanov, T. Claeson, O. Harnack, M. Darula, S. Beuven, and H. Kohlstedt, IEEE Trans. Appl. Supercond. **9**, 3761–3764 (1999).
[10]N. Bergeal, X. Grison, J. Lesueur, G. Faini, M. Aprili, and J. P. Contour, Appl. Phys. Lett. **87**, 102502 (2005).
[11]F. Kahlmann, A. Engelhardt, J. Schubert, W. Zander, C. Buchal, and J. Hollkott, Appl. Phys. Lett. **73**, 2354–2356 (1998).
[12]N. Bergeal, J. Lesueur, G. Faini, M. Aprili, and J.-P. Contour, Appl. Phys. Lett. **89**, 112515 (2006).
[13]S. A. Cybart, S. M. Wu, S. M. Anton, I. Siddiqi, J. Clarke, and R. C. Dynes, Appl. Phys. Lett. **93**, 182502 (2008).
[14]S. A. Cybart, S. M. Anton, S. M. Wu, J. Clarke, and R. C. Dynes, Nano Lett. **9**, 3581 (2009).
[15]N. Bergeal, J. Lesueur, M. Sirena, G. Faini, M. Aprili, J.-P. Contour, and B. Leridon, J. Appl. Phys. **102**, 083903 (2007).
[16]D. E. McCumber, J. Appl. Phys. **39**, 3113 (1968).
[17]S. Shapiro, Phys. Rev. Lett. **11**, 80 (1963).
[18]See supplementary material at http://dx.doi.org/10.1063/1.4769441 for more information on the dynamical range of the mixer and on the irradiation through slits of different widths.
[19]Y. Taur, IEEE Trans. Electron Devices **27**, 1921 (1980).
[20]M. Sirena, X. Fabreges, N. Bergeal, J. Lesueur, G. Faini, R. Bernard, and J. Briatico, Appl. Phys. Lett. **91**, 262508 (2007).
[21]M. Sirena, S. Matzen, N. Bergeal, J. Lesueur, G. Faini, R. Bernard, J. Briatico, D. G. Crete, and J. P. Contour, J. Appl. Phys. **101**, 123925 (2007).
[22]M. Sirena, S. Matzen, N. Bergeal, J. Lesueur, G. Faini, R. Bernard, J. Briatico, D. G. Crete, and J. P. Contour, Appl. Phys. Lett. **91**, 142506 (2007).
[23]M. Sirena, S. Matzen, N. Bergeal, J. Lesueur, G. Faini, R. Bernard, J. Briatico, and D. G. Crete, J. Appl. Phys. **105**, 023910 (2009).
[24]P. Barbara, A. B. Cawthorne, S. V. Shitov, and C. J. Lobb, Phys. Rev. Lett. **82**, 1963 (1999).
[25]M. Darula, T. Doderer, and S. Beuven, Supercond. Sci. Technol. **12**, R1–R25 (1999).